Direct flood risk assessment of the European road network: an object-based approach

Kees C.H. van Ginkel (1,2)*, Francesco Dottori (3), Lorenzo Alfieri (3,4), Luc Feyen (3), Elco E. Koks (2,5)

(1) Deltares, Boussinesqweg 1, 2629 HV Delft, The Netherlands
(2) Institute for Environmental Studies, VU University, Amsterdam, The Netherlands
(3) European Commission, Joint Research Centre, Ispra, Italy
(4) CIMA Research Foundation, University Campus of Savona, Savona, Italy
(5) Environmental Change Institute, University of Oxford, Oxford, United Kingdom

*Corresponding author: kees.vanginkel@deltares.nl

ORCIDs:

Kees van Ginkel: 0000-0002-8162-221X

Francesco Dottori: 0000-0002-1388-3303

Lorenzo Alfieri: 0000-0002-3616-386X

Luc Feyen: 0000-0003-4225-2962

Elco Koks: 0000-0002-4953-4527

Abstract

River floods pose a significant threat to road transport infrastructure in Europe. This study presents a high-resolution object-based continental-scale assessment of direct flood risk of the European road network for the present climate, using high-resolution exposure data from OpenStreetMap. A new set of road-specific damage functions is developed. The median expected annual direct damage from large river floods to road infrastructure in Europe is 250 million euro per year. Compared to grid-based approaches, the object-based approach is more precise and provides more action perspective for road owners, because it calculates damage directly for individual road segments, while accounting for segment-specific attributes. This enabled the identification of European hotspots, such as the Alps and roads along the Sava River. A first comparison to a reference case shows that the new object-based method computes realistic damage estimates, paving the way for targeted risk reduction strategies.

1 Introduction

River flooding is among the most damaging natural hazards in Europe. Following disruptive and costly European floods in the year 2000 and between 2009 and 2014, significant advances in continental (and global) scale flood risk modelling have been made (Dankers and Feyen, 2008; Hirabayashi et al., 2013; Kundzewicz et al., 2017; Ward et al., 2013). Although these models provide good estimates of total damage to all land use types, they do not accurately represent damage to

35   transport infrastructure (Jongman et al., 2012, Bubeck et al., 2019). Flood damage to road infrastructure is still an underexplored, yet important issue (Doll et al., 2014; Merz et al., 2010; Koks et al. 2019). Previous studies have shown that transport infrastructure significantly contributes to direct tangible flood losses, usually in the order of 5-10% but in exceptional cases up to 50-60% (Bubeck et al., 2019; Jongman et al., 2012). At the same time, transport disruptions are an important

40   source of indirect economic effects through passenger and cargo delay costs, which may exceed the direct costs (Pregnolato et al., 2017). Furthermore, the accessibility of the road network during flood events is of crucial importance to evacuations and therefore in avoiding casualties (Sohn, 2006). Vehicle-related drowning is the most frequent cause of death during flood disasters (Jonkman and Kelman, 2005). This study focusses on improving the estimates of direct physical damage to road

45   infrastructure, but also paves the way for assessment of indirect effects.

Existing continental-scale river flood risk studies do not accurately represent damage to road networks for several reasons. First, these studies are typically grid-based. Damage in a grid cell is determined using a depth-damage curve based on the land use and flood depth in each grid cell. In these grid-based approaches, infrastructure damage is typically determined using the (potential)

50   percentage of infrastructural land use in a cell. However, transport network infrastructure such as roads and railways are (relative narrow) line elements and take up only a small percentage within a typical grid size for continental-scale modelling (e.g. 100*100 m^2 in Europe). As these (assumed) percentages are often applied uniformly among the same land-use type, this may result in an overestimation of infrastructure damage when there in reality is no infrastructure, but an

55   underestimation if the infrastructure is there but not enough to be the dominant land-use type. Second, little progress has been made in research on transport-specific damage functions (Hackl et al., 2016). One reason is that damage to road infrastructure does not contribute much to the overall flood damage. Also, there is limited reported data on road damage from flooding. Many studies have pointed out that research on flood vulnerability is underdeveloped (Dottori et al., 2018a), with high

60   associated uncertainty (de Moel and Aerts, 2011) stressing the need for improved vulnerability methods (Winsemius et al., 2013), especially for infrastructure (Jongman et al., 2012). To date, virtually all European-wide flood risk studies (Bouwer et al., 2018, Dottori et al., 2020, Lincke et al., 2019) still rely on the comprehensive set of damage curves proposed by Huizinga (2007), which were developed for (coarse) grid-based assessments, but lack detail for accurate assessment of damage to

65   road networks (Jongman et al., 2012).

Previously, the grid-based approach could be justified by incomplete object-based exposure datasets, and insufficient computational power for a more detailed approach. Object-based transport infrastructure datasets such as OpenStreetMap are now nearly complete (Barrington-Leigh and Millard-Ball, 2017), and computational power is no longer a limiting factor, allowing for high-

70   resolution damage modelling approaches (Koks et al. 2019). Object-based damage models have substantial benefits compared to grid-based approaches. First, the geometric representations have a higher resolution, allowing for more accurate intersects between the exposed roads and the hazard data. Second, object-specific attributes can be used to make more accurate damage estimates (Merz et al., 2010). For example, for an intersect between the road network and an inundation map,

75   it is crucial to differentiate an inundated road from a bridge over the water. The attributes also enable the development of different damage curves for different road types (e.g. motorway or rural road), which may have very different characteristics (e.g. number of lanes, width, quality and maintenance standards). Third, the network properties of roads, enabling graph representations, can

be maintained in an object-based approach (Gil and Steinbach, 2008). This enables the study of direct infrastructural flood damage in coherence with other sources of impacts, such as travel delay times from road closures and detours, as well as indirect economic losses from passenger or freight delays.

Koks et al. (2019) proposed a method to study the impacts of climate hazards to road (and rail) infrastructure on the global scale, using data from OSM. The analysis in this global, multi-hazard study used highly stylized damage functions and had to take several assumptions due to information gaps in data-scarce parts of the world. In Europe, object attribute data availability is more complete, allowing for a more detailed approach in this study. Based on an extensive review of road (re)construction costs in Europe, we developed new damage curves by utilizing the available data on road type, number of lanes and the presence of street lighting. Also, we benefit from the higher resolution of flood protection and GDP data in Europe. The increased level of detail allows for presenting the results on the level of individual road segments for hotspot identification. This meets the need of European road owners for GIS-aided vulnerability assessments, for which guidelines have been provided in the ROADAPT project (Bles et al., 2016) but where actual modelling has so far focussed on small spatial scales (e.g. Hackl et al., 2018).

This study introduces an object-based, continental-scale assessment of large-scale river flood risk of the European road network for the present climate. We introduce new damage functions for the object-based approach and compare it to a grid-based approach. To illustrate the richness of the object-based approach, flood hotspots will be identified within the European motorway network. The model results are compared to damage reported for a real flood event near Deggendorf, Germany.

2   Method

Flood risk is commonly defined as a function of flood hazard, exposure and vulnerability (Kron, 2005; Peduzzi et al., 2009). In this study, these components are modelled in three blocks (Fig. 1). Hazard data are taken from the Joint Research Centre's inundation maps of large river floods in Europe (Fig. 1, left). The hazard maps are inputs to two approaches that model exposure and vulnerability: the traditional grid-based approach (Fig. 1, top) and the new object-based approach (Fig. 1, bottom). In total, four combinations of exposure and vulnerability are used to calculate the risk.

Grid-based:

1.   CORINE land cover + Huizinga infrastructure damage curve
2.   LUISA land cover + Huizinga infrastructure damage curve

Object-based:

3.   OpenStreetMap + object representation of Huizinga infrastructure damage curve
4.   OpenStreetMap + new object-based damage curves

These four combinations are selected to enable a comparison between the grid-based and object-based approach, for (1) a land cover grid with poor representation of the road network, (2) a land cover grid with the road network explicitly added to the grid, (3) an object-based approach with the damage curves from the grid-based approach, and (4) an object-based approach with new damage

curves. In the remainder of this section, we introduce the flood hazard maps (Sect. 2.1), the grid-based approach (2.2), the object-based approach including the development of new damage curves (2.3), and the reference case (2.4).
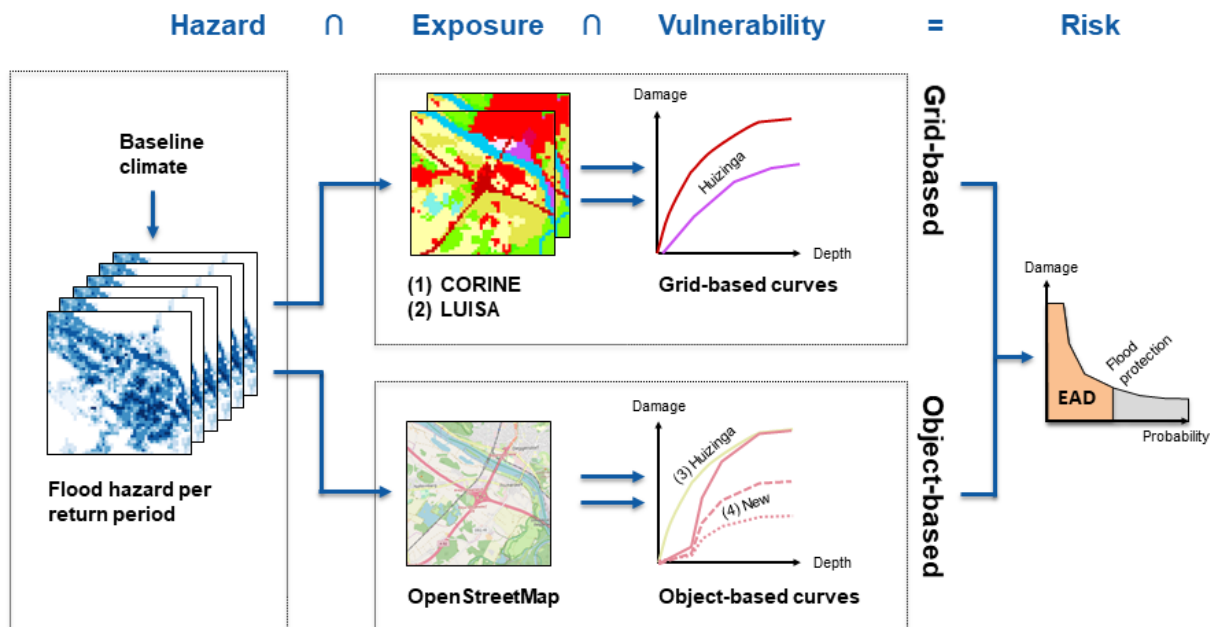
Figure 1 Graphical representation of the risk assessment using the grid-based approach (top-row) with the (1) CORINE and (2) LUISA land cover grids and the object-based approach (bottom-row) with OpenStreetMap and (3) the Huizinga and (4) a set of new damage curves © OpenStreetMap contributors 2019. Distributed under a Creative Commons BY-SA License

2.1   Flood hazard

Flood hazard is represented with a set of inundation maps taken from Alfieri et al. (2015), with a recent update by Dottori et al. (2020) which cover most of the European domain at a grid resolution of 100 m. The dataset consists of six inundation maps corresponding to flood return periods of 10, 20, 50, 100, 200 and 500 years, assuming no flood protection in place. These maps represent the inundation depth and extent in all river sections with upstream area larger than 500 km^2. They do not include the effect of pluvial flooding, coastal flooding, as well as river and flash flooding in the most upstream catchments. Inundation maps were produced by merging the results of thousands of 2D hydraulic simulations along the European river network, based on the hydrodynamic model LISFLOOD-FP (Bates et al., 2010). The input hydrographs of flood simulations were defined consistently with the peak discharges and flow duration curves of a 25-year long simulation taken from the European Flood Awareness System (Thielen et al., 2009) and based on the hydrological model LISFLOOD (Van der Knijff et al., 2010). Additional details on the methods and models used to produce the maps are described in Alfieri et al. (2014; 2015), together with some skill assessment of the simulated maps versus official regional inundation maps for the United Kingdom and Germany.

2.2   Grid-based exposure and vulnerability

In the grid-based approach, two different land cover maps are used: CORINE-2012 (version 18.5) and LUISA (version 2). They indicate the dominant land use type in each 100*100 m^2 grid cell. The CORINE land cover map (Büttner et al., 2014) and its predecessors have been used in many European flood risk studies (e.g. Alfieri et al., 2018; Lugeri et al., 2010; Serinaldi and Kilsby, 2017). CORINE, however, overlooks most of the road network (Rosina et al., 2018), because even large

motorways typically cover less than 50% of a 100*100 m^2 grid cell, see Fig. S2. Therefore, roads have been manually added to the land cover map in some studies (e.g. Jongman et al., 2012; cf. Meneses et al., 2019). The LUISA land cover map is a spatial and thematic refinement of CORINE-2012 using various additional data sources, such as rasterized object datasets (Rosina et al., 2018). Therefore, motorways and trunk roads that were absent in CORINE are now present in LUISA as coarse grid representations of the original lines. However, due to the resolution of the grid, the actual road width is overestimated in most areas (Fig. S2).

To correct for the underrepresentation of infrastructural land use (and other land use types) in CORINE and LUISA, they assume for each land use class some percentage of infrastructure (Table S1, 2). This assumption follows from Huizinga's suggestion (2007, p. 2-22) to map the damage functions to CORINE using a cross-tabulation by the EEA (2006), which then became the default implementation method. To enable a comparison with the object-based approach, we only consider the percentage of infrastructure per land use class, whereas the contributions of the other damage curves are ignored (Table S1, 2). An implication of these percentages is that, although motorways and trunk roads are mostly missing in CORINE, damage for (local) roads in urban and industrial areas (amongst others) is still calculated, albeit without any explicit spatial reference to the actual road position, but based on their average presence in these land use types. Also, note that in the land cover category 'road and rail networks and associated land', only a 27% infrastructural land use is assumed (Table S1, 2), which to some extents corrects the overestimation of the actual road widths in LUISA. In summary, the grid-based land cover category 'Road and rail networks and associated land' roughly corresponds to the object-based road types 'motorway' and 'trunk road', and the infrastructure percentages in the other grid-based land cover categories roughly correspond to the object-based road types 'primary', 'secondary', 'tertiary' and 'other road'.

2.3   Object-based exposure and vulnerability

This section details the set-up of the object based model (2.3.1); the estimation of the value of the exposed roads (2.3.2); the development of the new damage curves (2.3.3); the application of the Huizinga reference curve (2.3.4); and the sampling from the uncertainty spanned by the new damage curves (2.3.5).

2.3.1   Model set-up

In the object-based approach, all individual OSM road segments in Europe are intersected with the flood hazard data, followed by a damage and risk calculation per inundated segment (Fig. 2). To perform this analysis using parallel processing (Fig. 2), the continental OSM 'planet' file is subdivided into 1498 regions[1], based on the European NUTS-3 division. Per region, every road segment is intersected with the flood hazard maps per return period, to determine the inundated length and average depth over the inundated part of the segment. Then, the damage to the road segment is calculated for the applicable damage curves. In the post-processing step, the expected annual damage (EAD) is calculated using the trapezoidal rule (Olsen et al., 2015), accounting for flood protection (Fig. S1). Flood protection data is derived from the dataset developed by Dottori et al.

---

[1] For hydrological reasons, our analysis includes the European Union (EU) 27 member states except Cyprus and Malta; it includes the United Kingdom and the adjacent European Free Trade Association countries Liechtenstein, Norway and Switzerland (not Iceland); and includes the (potential) candidate countries Albania, Montenegro, North Macedonia and Serbia (not Turkey). We excluded the EU's remote overseas areas such as the Azores, Canary Islands, Guadeloupe as well as small Islands.

185   (2020). The dataset integrates the available information on design standards of flood protection (e.g. through technical reports) with modelled protection standards calculated by Jongman et al. (2014) and Scussolini et al. (2016). Modelled data is selected according to observed and simulated historical flood loss data. In this step, the maximum damage per segment is corrected by linearly scaling the national to the former EU-28 average real GDP per capita (Eurostat, 2019).

190
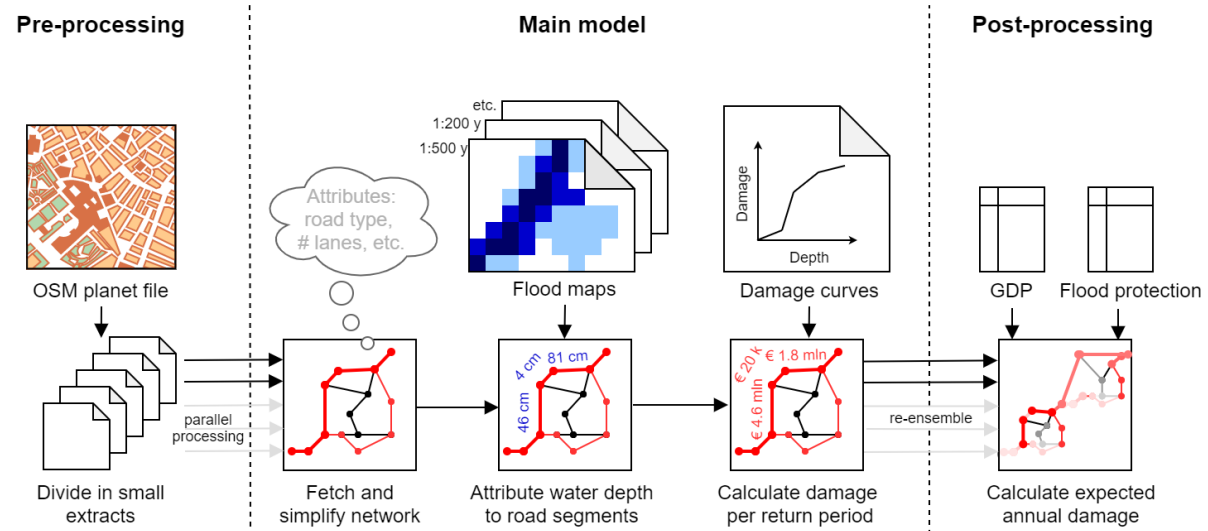
Figure 2 Stylized overview of the object-based approach

Where available, OSM attributes on road type, number of lanes, bridges and lighting is used to improve the damage estimates. Six road types are distinguished following the OSM tagging
195   convention[2]: motorway, trunk, primary, secondary, tertiary and other roads (Table S3). Lane data is available for 90% of the motorways, 60% of trunks, 48% of primary, 23% of secondary, and less than 5% for tertiary and other roads; where unavailable, the countries' median number of lanes per road type is used. For road-water intersections tagged as bridges, no damage to the road is calculated. We acknowledge that bridge failure can be an important source of flood damage (Lamb et al., 2019;
200   Pregnolato, 2019; Vennapusa et al., 2013). Bridge damage, however, does not usually originate from the inundation of the roadway, but rather from scour hole formation to bridge piles and its foundation (Lamb et al., 2019), which cannot be accurately represented in our model.

2.3.2   Overview of road construction costs

To construct the new damage curves, we compile an overview of road construction, maintenance
205   and repair costs. These costs are related to the road repairs needed following a river flood, derived from literature and photo imagery of river floods in Europe. The damage narratives and resulting curves are validated during an expert workshop with flood risk and transport modelling experts and with the Dutch road operator, see acknowledgements. An overview of the damage curves and supporting narratives (reasoning from the road construction and maintenance costs presented

---

[2] Key: highway. (6 February, 2019). In *OpenStreetMap Wiki*. Retrieved April 18, 2019, from
https://wiki.openstreetmap.org/wiki/Key:highway

210   below) is given in Fig. S3, 4 and Table S9, 10. The damage curves cover what it would cost for the road operator to have the road cleaned and repaired by a contractor. It includes clean-up costs, resurfacing of top and deeper asphalt layers, repairs of road embankments, and where applicable also the repair of electronic signalling and lighting. It does not include structural damage to bridges and tunnels, nor emergency response costs such as the placement of sand bags or signposting of
215   diversions.

All costs mentioned in this and the following subsection are linearly scaled using national real GDP per capita (Eurostat, 2019) to represent former EU-28 average, 2015 price-levels in euro (€). The model inverses this operation when doing the damage calculation, to tailor the damage to the local context. This is common practice in pan-European flood risk studies (e.g. Alfieri et al., 2016b; Arnell
220   and Gosling, 2016; Ward et al., 2013) and enables comparison with existing studies. Besides GDP, the cost of constructing a new road depends on many factors, such as: road design; accessories like lighting and electronic signalling systems; soil conditions; noise reduction elements; and presence of tunnels and bridges (e.g. Blanc-Brude et al., 2006). For *motorways*, the European Court of Auditors (ECA, 2013) estimates the EU average construction costs at 11.4 million €/km. The cheapest 2x2 lane
225   motorways with fairly simple road designs are about 3.5 million €/km, the most expensive roads with tunnels, bridges or noise barriers cost about 35 million €/km (ECA, 2013). Other studies report values well within this bandwidth (Carruthers, 2013; Federal Ministry of Transport and Digital Infrastructure, 2016; Heralova et al., 2014; Nijland et al., 2010; Pryzluski et al., 2012), as presented in Table S6. For costs of other road types see Table 1, which is based on literature tabulated in the SI
230   (Table S5-7). For roads with more (less) than the default number of lanes, we added (subtracted) 25% of costs for each lane, based on Table S5.

2.3.3   Estimating the shape of the damage curves

Continental-scale models typically work with functions relating damage to water depth only (Alfieri et al., 2016a; de Moel et al., 2015; Winsemius et al., 2013). Flow velocity, however, is at least as
235   important as water depth for explaining damage to roads (Kreibich et al., 2009; Merz et al., 2010; Thieken et al., 2009). Under low flow velocities (< 0.2 m/s), there is hardly any structural damage to pavements, whereas under high flow velocities (> 2.0 m/s) there is most likely severe structural damage (Kreibich et al., 2009). Indeed, pictures of floods in Europe show that under very quiet flow conditions, a road can remain almost undamaged whereas under flash floods with strong currents,
240   complete reconstruction may be required. The flood hazard maps used in this study represent floods in rivers with an upstream area >500 km^2 whereas large flow velocities are typically found in smaller water courses in steep upstream areas and locally, close to dike-break locations (De Moel et al., 2009). Therefore, we assume that the predicted floods have relatively low flow velocities. We deal with the remaining uncertainty by estimating two depth-damage curves that span the uncertainty of
245   this typical slow flow velocity; one for the low-flow estimate and one for high-flow estimate that can be reasonably expected for large river floods.

The six new depth-damage curves differentiate between three dimensions: road type, road accessories and flow velocity (Figure 3). Concerning road type, motorways and trunk roads are distinguished from other roads because of higher driving speeds and maintenance standards, reflected in higher reconstruction costs. Also, these are often built on top of embankments, so that relatively little damage occurs when the top of the road embankment is not yet reached, represented by a concave section in the beginning of curve C1-C4. The other road categories

(primary, secondary, tertiary and other roads) are usually not built on top of embankments, and their curves (C5,C6) therefore do not have such a concave section. Next, motorways and trunk roads with sophisticated accessories such as electronic traffic management systems, lighting and noise barriers (C1,C2) are differentiated from simple roads without these accessories (C3,C4). This represents the large spread in construction costs between simple and sophisticated motorways and trunk roads (Table S6) and the corresponding extra damage that may occur to the electronic signalling and lighting of sophisticated roads, even under low-flow conditions. Finally, low-flow conditions (C1,C3,C5) are distinguished from high-flow conditions (C2,C4,C6).
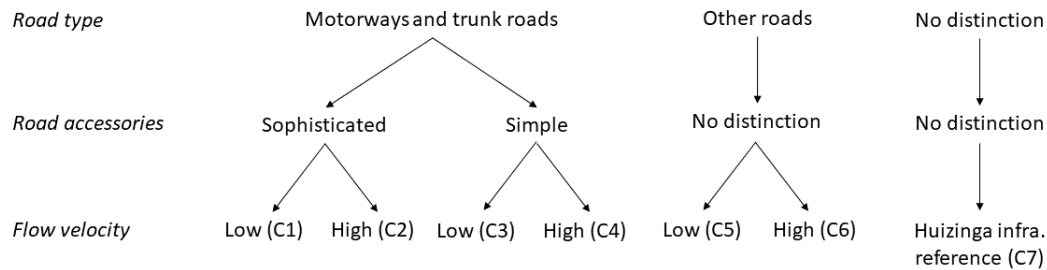
Figure 3 Dimensions used for differentiating the new damage curves (C1-C6) and the reference curve (C7)

Road maintenance and repair costs (Table S8) are used for estimating flood damage under various flood depth and velocity conditions. These are expressed as a percentage of the construction costs of the corresponding road type. For example, for roads without embankments, clean-up and small repair works are in the order of a few percent of construction costs (Reese, 2003, Archondo-Callao, 2000) and are required for small flood depths (<50 cm) with low velocity. Larger scale road improvement and resurfacing is in the order of 10% of construction costs (Carruthers et al., 2013, Archondo-Callao, 2000). Major asphalt works and road reconstruction is in the order of 30-40% of construction costs (Carruthers et al., 2013; Archondo-Callao, 2000), and is required for larger flood depths and higher flow velocity (Table S9, S10).

Table 1 Road construction costs and maximum damage per road type, differentiated between low flow (low flow velocities) and high flow (high flow velocities). The values present the average for the former EU-28, in million 2015-euro per km.

Road type	Lanes [-]	Construction cost range [10^6 €/km]	Max damage (low flow) [-]	Max damage (high flow) [-]	Max damage (low flow) [10^6 €/km]	Max damage (high flow) [10^6 €/km]	Huizinga max dam.[A] [10^6 €/km]
			Relative to constr. costs		Absolute values		
Motorway	2*2	3.5 - 35	20% (a)[B] 4% (s)[B]	22% (a)[B] 35% (s)[B]	3.9-7.0 (a)[C] 0.1-0.8 (s)[C]	4.2-7.7 (a)[C] 1.2-6.7 (s)[C]	0.90
Trunk	2*2	2.5 - 7.5	20% (a)[B] 4% (s)[B]	22% (a)[B] 35% (s)[B]	1.0-1.5 (a)[C] 0.10-0.20 (s)[C]	1.1-1.7 (a)[C] 0.88-1.75 (s)[C]	0.60
Primary	2*1	1.0 - 3.0	5%	35%	0.050-0.150	0.350-1.050	0.25
Secondary	2*1	0.50 - 1.5	5%	35%	0.025-0.075	0.175-0.525	0.225
Tertiary	2*1	0.20 - 0.60	5%	35%	0.010-0.030	0.070-0.210	0.175
Other	1	0.10 - 0.30	5%	35%	0.005-0.015	0.035-0.105	0.075

Notes:

A) Huizinga max damage costs [€/km] are obtained by multiplying the m^2 costs with typical road widths per road type (Table S4).

B) a = road with accessories such as street lighting and electronic signalling; s = simple road, without accessories

C) For accessories roads: 50-100% of the construction costs range, for simple roads: 0-50% of the construction costs range

2.3.4 The Huizinga reference curve

A comprehensive set of depth-damage curves has been proposed by Huizinga et al. (Huizinga, 2007; Huizinga et al., 2017), which has been applied in many studies (e.g. Albano et al., 2017; Amadio et al., 2016, 2019; Carisi et al., 2018; Dottori et al., 2018b; Jongman et al., 2012; Prahl et al., 2018). We use the 'EU-average curve' for road infrastructures (Huizinga, 2007) to compare to our new curves. In this study, the curve is used in both the grid-based approach and the object-based approach, where the per m^2 damage was multiplied by typical widths of roads in Europe (Table S4).

2.3.5 Sampling the uncertainty space

The damage estimates come with considerable uncertainty, which primarily originates from the bandwidth of the maximum damage estimates and the space between the upper and lower estimate of the flow velocity. This uncertainty space is sampled to obtain (1) a deterministic estimate of the expected annual damage, as well as (2) a probability distribution around a median estimate. Motorways and trunk roads with street lighting tags in OSM are assumed to have sophisticated road accessories; damage curves C1 and C2 are applied (Fig. 3) in combination with a max damage sample from 50-100% of the max damage range (Table 1, note C), and 75% in the deterministic sample. For motorway and trunk roads without street lighting tags, simple road designs are assumed; damage curves C3 and C4 are applied in combination with a sample from 0-50% of the max damage range, and 25% in the deterministic sample. Concerning the uncertainty in flow velocity, we assume a normal distribution with the low flow curve at -2 standard deviations and the max flow curve at +2 standard deviations from the mean flow damage, and the average of the min and max flow curve in the deterministic estimate.

2.4 Comparison to reference case

As a reference, we compare our model to road repair data reported by the Bavarian Government (Table S17). On 4 and 5 June 2013, an approximately 1:100 year flood caused a dike breach near the confluence of the River Danube and its tributary: the River Isar, close to the town of Deggendorf. The inundated area spanned the cloverleaf junction of the motorways A92 and A3, as well as 6.6 km of the A3 and 2.8 km of the A92 (Fig. 7). Both roads have 2*2 lanes + 2 safety lanes and are 30 m and 26 m wide, respectively. The roads are located on embankments and have a fairly simple road design, i.e. no lighting or electronic signalling. We estimate water depths and damage to these roads and surrounding area from reports (Rogowsky, 2016), video's, photos and satellite imagery (Table S17). We then mask the 1:10 year flood hazard map (which better resembled the reported inundation than the 1:100 year flood map) over the extent of the observed inundation and calculate the damage using the object-based model.

3 Results

This section presents the flood risk of the European road network. Firstly, the new object-based approach is compared to the grid-based approach, using the same damage curves in both approaches (Sect. 3.1). Secondly, the new damage curves are used in the object-based approach, to give more precise estimates of the aggregated road damage in Europe and to give insight into the uncertainty surrounding these estimates (3.2). Thirdly, these results are presented on the road segment level to identify flood hotspots in the European highway network (3.3). Fourthly, the model results are validated by comparison with the damage reported for the Deggendorf flood event (3.4).

3.1 Grid-based vs. object-based damage for Huizinga damage curve

The grid-based approach estimates the total expected annual damage (EAD) for the CORINE and LUISA land cover map at 536 and 301 million €/y respectively (Fig. 4a), whereas only 228 million €/y is estimated by the object-based approach (Fig. 4b). Both approaches use the same hazard data and both use the Huizinga vulnerability curve, so that the differences are mainly attributable to the exposure data. A surprising observation concerning the exposure data is the large amount of infrastructural damage (65%) attributed to the CORINE land cover type 'water'. This peculiarity originates from Huizinga's suggestion (Huizinga, 2007, p. 2-22) to map the damage functions to CORINE using a land cover cross-tabulation from the European Environment Agency (EEA, 2006, cf. Table S1). The EEA shows that some cells that contain 'water bodies' in CORINE contain 'infrastructure' in a reference map. Consequently, some percentage of infrastructure is assumed for all CORINE water bodies, for which large damage is calculated, because sometimes large 'inundation depths' are modelled for water bodies. This peculiarity was manually removed in the model implementation of LUISA (Table S2), such as in the recent PESETA-IV study (Dottori et al., 2020). Another difference between CORINE and LUISA is the strong increase in damage to 'Road and rail networks and associated land', from 15 to 144 million €/y respectively, resulting from integrating the motorway network into the LUISA land cover grid (Rosina et al., 2018).

It should be noted that the object-based approach only reports damage to road infrastructure, whereas the grid-based approach also reports damage to rail infrastructure. However, since railways are very narrow line elements and have not been explicitly integrated in the LUISA grid (Rosina et al., 2018), their contribution to the LUISA damage is small. Therefore, we assume that LUISA class 'Road and rail networks and associated land' corresponds to the motorway network and that the other LUISA land use classes correspond to the underlying road network. Accordingly, in the grid-based approach, motorways contribute 48% and the underlying road network 52% to the total road infrastructure damage (Fig. 4a). In the object-based approach, motorways contribute 9%, trunk roads 7%, and the underlying road network 85% (Fig. 4b). This relatively minor contribution of motorways in the object-based approach results from the way in which the Huizinga curve is implemented: damage per square meter is multiplied by the road width. Motorways, however, are more expensive than is to be expected from merely their width. Therefore, the damage to motorways is underestimated in Figure 4b. The other way around, the other road types are less expensive than is to be expected from their width. Therefore, damage to the underlying road network is underestimated in Figure 4b. This emphasizes the need for damage curves that correct for road characteristics beyond only the road width, as used in the next section.
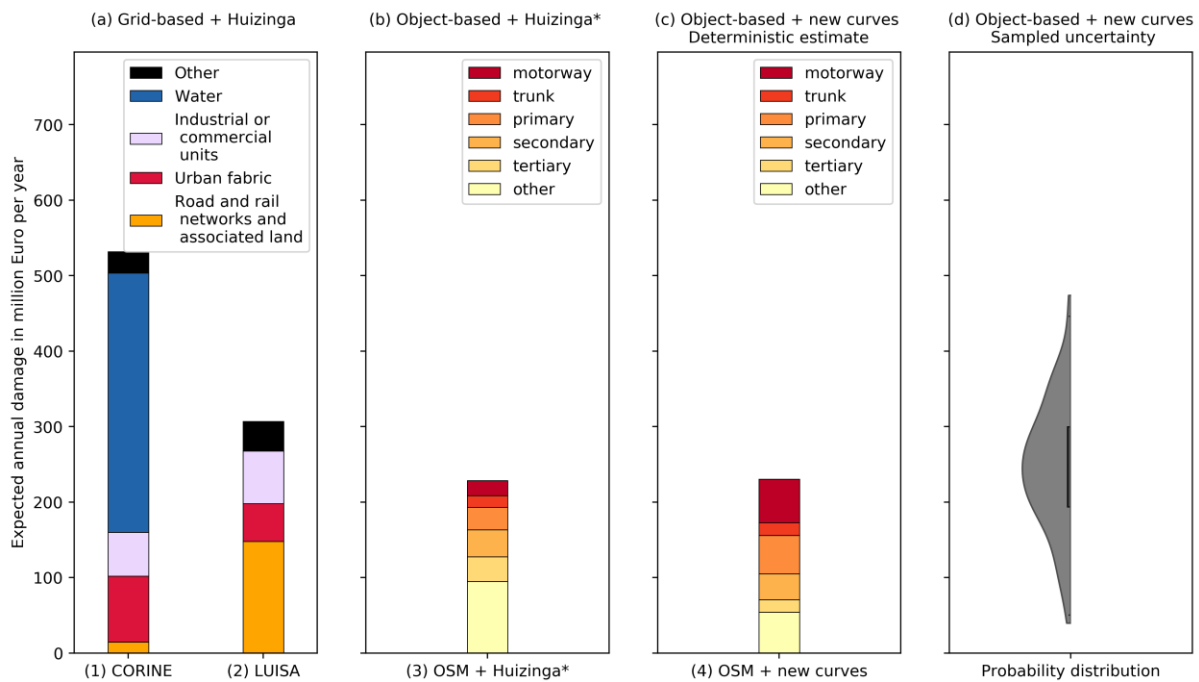
Figure 4 Flood risk of the European road network according to the grid-based and the object-based approach
(a) Grid-based approach with (1) CORINE and (2) LUISA + the Huizinga damage curves, per land cover type
(b) Object-based approach + *object translation of Huizinga damage curves (3), per road type
(c) Object-based approach + new damage damage curves (4), deterministic estimate per road type
360 (d) As (4) with probability density around the deterministic estimate of panel c, black line indicating the interquartile range

3.2   Object-based damage using new damage curves

With the new depth-damage curves the EAD is estimated at 229 million €/y (Fig. 4c), which is again below the grid-based LUISA estimate (301 million €/y, Fig. 4a). The total damage with the new curves (229 million €/y, Fig. 4c) is almost the same as the object-based implementation of the 365 Huizinga damage curve (228 million €/y, Fig. 4b), but the contribution per road type is substantially different. Notably, the contribution of motorways (25%) has become much larger. The other contributions are 7% for trunk, 22% for primary, 15% for secondary, 7% for tertiary and 24% for other roads (Fig. 4c)

The object-based approach also gives insight into the uncertainty surrounding the deterministic 370 estimate of 229 million €/y. Fig. 4d shows the bandwidth derived from the sampling procedure (Sect. 2.3.5). The median of the stochastically generated samples is 250 million €/y, which is above the deterministic estimate of 229 million €/y, because on the upper bound, outliers in high flow velocities cause large damage, which is not compensated at the lower bound because the damage per segment cannot be lower than zero. The interquartile range (containing 50% of the samples) is 375 195 to 301 million €/y, and the 90% range is 115 to 385 million €/y.

Figure 5a shows how the object-based risk (deterministic estimate) is geographically spread over Europe. Germany, France, and Italy are exposed to the highest flood risk (respectively 45, 43, and 23 million €/y, see Fig. S6,7). In these countries, the risk is concentrated around the rivers that rise in the Alps and then flow through regions with dense road networks, such as the Danube and Rhine 380 flowing through Southern Germany; the Rhone flowing through south-eastern France; and the Po flowing through northern Italy. These three countries have additional flood hotspots in the Elbe,

Garonne, and Tiber River basins respectively. Of the top-10 NUTS-2 regions with the largest damage, five are in France and two in Italy (Table S16).

Another concentration of high flood risk is found on the Scandinavian peninsula. This can be partly
385 explained by the high GDP per capita and the relatively large NUTS-regions. However, also when correcting for these factors, we find that the sparse road networks in these countries indeed have the potential to be inundated with large water depths, causing large damage. The regions Pohjois-ja Itä-Suomi (Finland) and Hedmark og Oplland (Norway) are in the top-10 of NUTS-2 regions with the largest risk (Table S16).

390 Because the value of the exposed assets is scaled to the national GDP per capita, the risk is relatively high in high-income countries. Without this GDP-correction, other high-risk countries emerge: the Central- European countries Czech Republic, Slovakia, and Hungary, but also Croatia and Latvia (Fig. 5a). Although these countries contribute little to the total damage in Europe, the relative impact of road disruptions in these countries is large. These regional risk aggregations are influenced by the
395 size of the regions in the NUTS classification; smaller regions show relatively smaller risk in Figure 5a. Therefore, aggregation at different levels reveals slightly different spatial patterns (Fig. S7, Table S14,15,16).
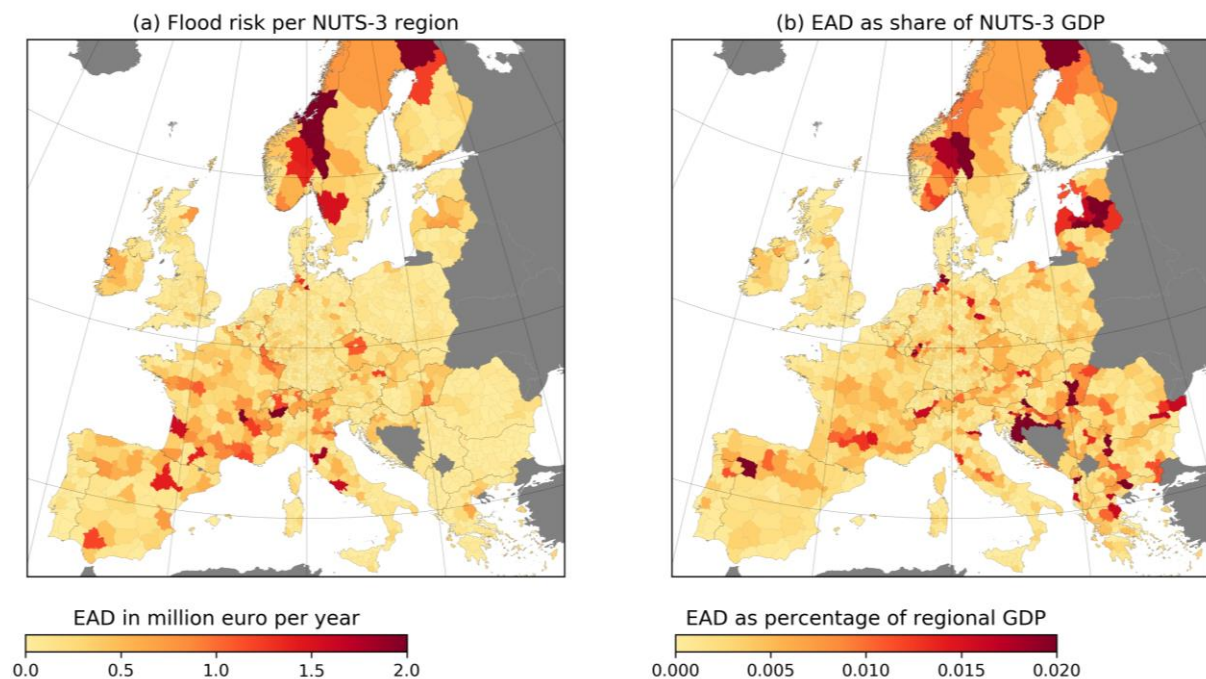
Figure 5 Expected annual damage (EAD) to road infrastructure aggregated by NUTS-3 region. The left-hand panel
400 **presents the absolute values, the right-hand panel expresses the EAD as percentage of the GDP per NUTS-3 region.**

3.3   Current flood hotspots in the EU transport network
The flood risk of all motorways and trunks in the EU road network is now presented on a high-resolution map, see Fig. S9. To illustrate how this map can be used to identify flood hotspots in the EU road network, we highlight three notable regions (Fig. 6).

405
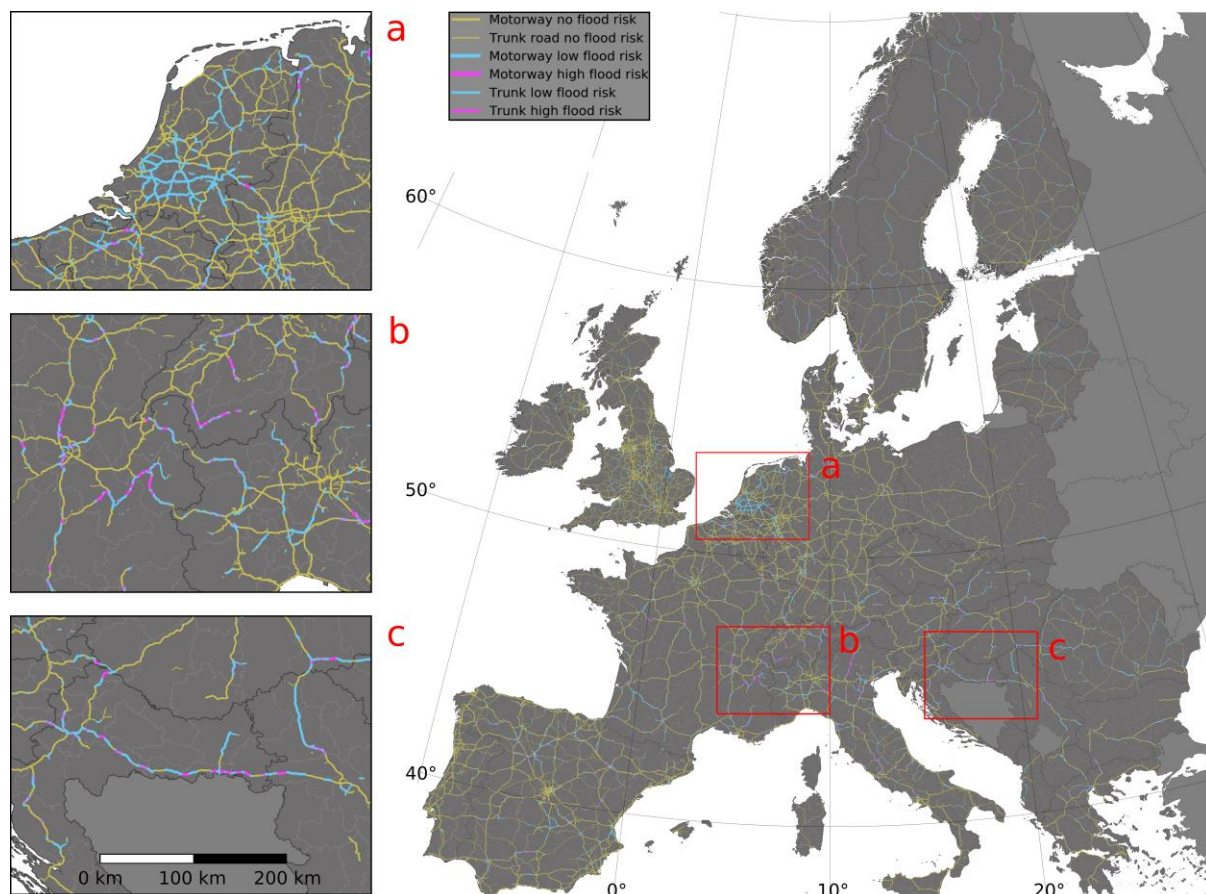
Figure 6 Flood risk of motorways and trunk roads in the European main road network, see Figure S9 for a high-resolution version. Road geometries © OpenStreetMap contributors 2019. Distributed under a Creative Commons BY-SA License.

The Netherlands stands out in Fig. 6a, because many of its motorways have the potential to be inundated, although at the same time, the aggregated flood risk is among the lower countries in
410 Europe (Fig. S6). This can be explained by the very high river flood protection standards in the country (return period of 1:1000 year or higher in most places), which make the likelihood of flood events very small. However, if dikes did breach, many roads would be inundated with large water depths, causing large damage. Also, this could severely hinder the possibilities for evacuation, especially in the centre of the country.

415 The Alps are identified as a high-risk region. For example, in France, the model predicts large EAD for the A41 from Grenoble to Chambéry, and the A43 from Chambéry to Sain-Jean-de-Maurienne (Fig. 6b). Both motorways are located in narrow flood plain valleys along rivers. This exposes them to large flood hazards, which is also recognized in local flood risk studies (e.g. Strappazzon and Pierlot, 2017). Similar exposure of motorways can be found in other Alpine regions, such as the A9 from Sion
420 to Montreux (Switzerland), the A22 from Lake Garda to Bolzano (Italy), and the A12 from Landeck via Innsbruck to Kufstein (Austria).

In the Balkans, the E70 motorway from Zagreb (Croatia) to Belgrade (Serbia) is subject to large flood risk (Fig. 6c). This road follows the course of the Sava River for about 400 km. The flood plains of the Sava River were struck by a large flood in 2014 (International Sava River Basin Commission, 2014).
425 According to our model, the flood waters could hit the motorway at several locations. For some road segments the EAD is notably high. This is primarily the result of a large flood hazard rather than a

large value of exposed assets, because the GDP of Croatia and Serbia is below the (former) EU-28 average.

3.4   Deggendorf reference case

430   As described in Sect. 2.4, the Deggendorf flood event is used to validate the damage estimates of the model (Fig. 7). During the flood event, the pavement of the A3 was submerged over 6.6 km because the road embankment was lower than the water level in the surrounding area, resulting in water depth of 0.5 m above the road pavement, on average. After the flood, the A3 was covered with debris (a gas tank, hay bags covered in plastic, wooden logs, plastic bags, pallets), sand, and mud,

435   requiring a major clean-up. At the cloverleaf, there were rifts in the asphalt, requiring small asphalt works. Small strips of asphalt (but not the entire road) were milled and resurfaced. The embankment of the A92 was higher than the embankment of the A3, so that its pavement remained dry over the entire 2.8 km, except a small depression at an underpass with a local road (see Table S17).
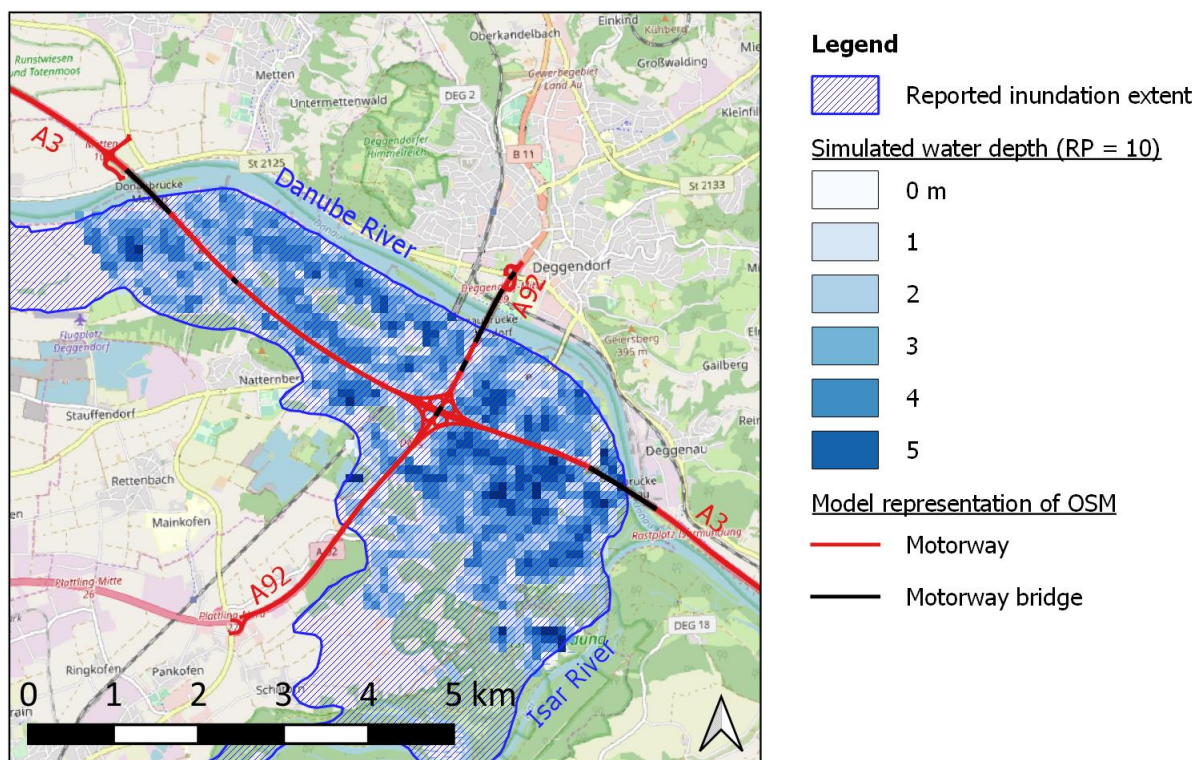
440   **Figure 7 Observed and simulated flood in Deggendorf.** Simulated map according to the cropped Return Period (RP) = 10 year flood map (Alfieri et al., 2015), background map © OpenStreetMap contributors 2019. Distributed under a Creative Commons BY-SA License.

The Bavarian State Ministry was granted 3.8 million euro for rehabilitating the Deggendorf cloverleaf junction (Table S17). The model calculates damage of 3.4 million for the low-flow curve (C3) and 28.6

445   million for the high-flow curve (C4). The video imagery and the limited asphalt damage (Table S17) suggest that flow velocities were relatively low, so that one expects the damage more towards our low-flow than the high-flow damage curve, which is indeed the case.

When interpreting these results, one should consider that German motorways are relatively cheap compared to those in other EU countries (after scaling for GDP, see Table S6); which could imply that

450   rehabilitation works are also relatively cheap (cf. ECA, 2013). Additionally, most damage seems to have occurred to the cloverleaf itself, rather than the straight sections of the two highways. Finally,

it is likely that the road owner made additional repair costs beyond what was funded using the 3.8 million euro grant.

4   Discussion

In this work, the object-based approach resulted in lower damage estimates than the grid-based approach. This contrasts with findings of previous studies. For example Jongman et al. (2012) found that "even with the complementary infrastructure data added to CORINE (by adding the road network to the grid), all damage models that include this class *strongly underestimate* the corresponding losses" (2012, p. 3744, brackets and emphasis by us) and that this "is in line with results from earlier studies" (p. 3748). Instead, our findings suggest that grid-based studies using CORINE may *overestimate* infrastructural damage by allocating infrastructural damage to water bodies. However, since the infrastructure contribution to the total damage in these approaches is limited, the estimate of total damage (beyond infrastructure) could still be reliable despite the misallocation in some land cover categories. The grid-based approach using LUISA provided an estimate close to the object-based assessment, indicating that with LUISA, a fair proxy of the total damage to road infrastructure can be obtained.

Within the object-based approach, replacing the Huizinga damage curve with a new set of damage curves resulted in a comparable estimate of the total road damage but distributed a larger share of the damage to motorways and trunk roads. This indicates that the Huizinga infrastructure function is a fair proxy for the average damage to road assets but is unsuitable for assessing damage at the individual road level. The Deggendorf reference case showed that the low-flow curve best resembled the reported flood damage. The new curves also compare reasonably well to damage reported for a Missouri River flood in in Iowa, United States of America (Vennapusa et al., 2013). In order to compare our curves to the damage reported in this study, let us assume a motorway construction costs of 5 million €/km, given that the road design in Iowa is fairly 'simple' (Table 1). Vennapusa et al. report the following motorway damage (Table S18): for clean-up costs: 18,000-65,000 €/km, which is in the order 1% (of 5 million €); for minor up till major repair works: 54,000-388,000 €/km, which is in the order of 1-10%; and for complete reconstruction of a motorway: 5.8 million €/km, which is in the order of 100% of construction costs.

European flood risk studies estimate the total river flood risk aggregated over all land cover types at 4-6 billion €/y (Alfieri et al., 2016b; Jongman et al., 2014), which resembles the reported damage (Paprotny et al., 2018). Our estimate of road damage of 250 million €/y is in the order of 4.2% (of 6 billion) to 6.3% (of 4 billion) of total damage. This infrastructure share of total flood damage is usually in the order of 5-10% (e.g. Pardoe, 2011, as cited by Jongman et al., 2012). Using grid-based models, Jongman et al. find 8.9%, 2.6% and 8.9% for a flood in Carlisle, for which 11.9% was reported. In specific cases, the damage may be much higher: Jongman et al. also find values of 18%, 5%, 17% and 3% for a flood in Eilenburg, for which 50% was reported. This made Bubeck et al. (2019) suggest that infrastructural losses may amount up till 60% of total damage. Our results however, suggest that such a high value should be seen as an exception; usually the infrastructure percentage of total damage is much lower. We also perceive Bubecks et al.'s estimate for the damage to railway infrastructure (11% - 14% of overall flood losses) as being on the high side, given that we find a percentage of only 4-6% for road infrastructure (with the same hazard data) and given that rail damage is usually smaller than road damage (Doll et al., 2014).

Our estimate of 250 million €/y, and 90% confidence interval of 115-385 million €/y is lower than the
660 million €/y reported by Enei et al. (2011). They used an elasticity model linking meteorological
indices to road vulnerability data derived from literature. This accounted for the aging of
infrastructure, so that the costs attributed to flood damage are lower than the unit replacement
costs. However, they included damage caused by landslides as well as damage to bridges, whereas
we only look at the impact of floods, and excluded damage to bridges.

Considering that other studies find higher values, could we have underestimated the damage? On
the one hand, this seems not to be the case. Firstly, the estimated size of total damage costs for the
reference event is at the lower range of our damage estimate. Secondly, it can be argued that places
for which our model calculates large damage could be more flood-proofed than what was
incorporated in our damage curves. For example, large damage is found for roads along rivers,
located in flat flood plains between mountains. In these very vulnerable places, the design standards
of the roads may be higher than of the average European road; the road could be extra protected in
anticipation of the flood events. Thirdly, road segments that follow a meandering river are
sometimes accidently intersected by the relatively coarse flood hazard grid, whereas they do not
flood. This makes our model more likely to overestimate than to underestimate the damage.

On the other hand, there are reasons to think that the actual river flood damage is larger than
predicted by our model. Firstly, we have limited ourselves to large river floods represented in the
flood hazard maps, thereby omitting floods originating from small catchments (<500 km^2). In hilly
terrain, flash floods and associated landslides in these smaller catchments can locally cause large
damage to road infrastructure, not the least because the flow velocities may exceed what was
anticipated in our high-flow curve. Secondly, our study omitted additional damage originating from
junctions, viaducts, bridges and tunnels, whereas these could contribute significantly to overall
damage. For the reference event, damage to the cloverleaf seems to have contributed most to the
overall damage. Similarly, a main source of the exceptionally large damage for the Eilenburg case
reported by Jongman et al. (2012) was the collapse of a bridge.

5   Conclusion

This study introduced a new object-based approach to modelling the river flood risk of European
road infrastructure. This enabled a comparison with the commonly used grid-based approaches,
which clearly have difficulties to accurately estimate damage to line infrastructure: road
infrastructure may either be overlooked or overestimated by attributing infrastructural damage to
the wrong land use types. Also, the study introduced a new set of damage curves which puts the
frequently used Huizinga curves in perspective. The median expected annual damage from river
floods to the road network is 250 million €/y, which is well below the grid-based estimates with
CORINE (536 million €/y) and LUISA (301 million €/y). Additionally, we showcased how the object-
based approach can be used to identify flood hotspots in the European road network, for which the
grid-based approach was unsuitable. This generalized approach can also be used for other hazards
such as coastal and pluvial floods. We especially recommend the investigation of the damage caused
by flash floods and associated landslides in hilly terrain, because the flow velocities and resulting
damages seem to exceed what we observed for large scale river flooding.

535   The model introduced in this study could be a starting point for further analysis. First, the flood hazard data can be easily substituted with (smaller-scale) high-resolution data, to fully exploit the level of detail offered by the OSM exposure dataset. In combination with higher-resolution flood hazard data, it is worth to investigate if splitting the OSM road segments in smaller subsegments can further improve the object-based approach. Second, local scale case studies are required to validate
540   the proposed damage curves. Currently, very little road flood damage case studies are described in the literature, collection of such data by road operators and academia should be a research priority because the absence of damage data hampers the validation of the models. Third, because road flood damage is very sensitive to uncertainty in flood velocity, accounting for this parameter could improve the predictive capacity of the model. Fourth, an object-based approach can be used to
545   investigate potential damage to bridges, culverts, tunnels, viaducts and junctions.

      In the broader context of risk assessments for roads, this study offers a practical method for large (continental) scale risk assessment without compromising the resolution of the exposure data, hence suitable for hotspot identification. Both continental scale and local scale assessments can use the same framework, only the hazard data needs to be substituted with high-resolution local data.
550   The results are presented on the level of individual road segments which meets a demand of road owners (Bles et al., 2016) by providing immediate perspective of action. This bridges the gap between detailed local-scale object-based studies (e.g. Hackl et al., 2018) and coarse continental-scale econometric (e.g. Doll et al., 2014) or grid-based studies (e.g. Dottori et al., 2020). Finally, the object-based approach offers an indispensable level of detail for two types of analysis. First, damage
555   from network disruptions and indirect economic effects can be studied using the same road network as used in the analysis of direct damage. Network graphs can be directly constructed from the OSM road objects, which is impossible with a grid-based approach. Second, flood risk studies are increasingly used to support decision making on climate adaptation. The unique characteristics of each road segment are highly relevant for targeted climate resilient infrastructure investments and
560   can only be captured in a road specific, object-based approach.

Supplementary information

      This paper contains supplementary information with model settings, road construction and maintenance cost data, the new damage curves, and detailed descriptions of the model results. These results include a high-resolution map and shapefile of the flood risk of motorways and trunk
565   roads in the European road network.

Code and data availability

      The Python code for the object-based model can be retrieved from github.com/keesvanginkel/OSdaMage. The SI contains a shapefile with the model outputs for the European highway network (motorways and trunk roads). Data for all OSM road classes per NUTS-3
570   region can be retrieved from the authors.

      The JRC flood hazard maps used in this work can be obtained upon reasonable request from Francesco Dottori (francesco.dottori@ec.europa.eu) and Luc Feyen (luc.feyen@ec.europa.eu). A previous version is available for download and reuse at the JRC Data Catalogue at this link: https://data.jrc.ec.europa.eu/collection/id-0054 .

Funding

This paper has received funding from the European Union's Horizon 2020 research and innovation programme under grant agreement No 776479 for the project CO-designing the Assessment of Climate CHange costs. https://www.coacch.eu/

Author contribution

KvG prepared the manuscript with contributions from all co-authors. FD, LA and LF prepared the flood hazard maps and damage maps of the grid-based approach. EK developed the object-based approach, KvG tailored it to the European context. KvG and EK carried out the computational experiments and investigated, validated, and visualised the results. All authors approved the final publication.

Competing interests

The authors declare that they have no conflict of interest.

Acknowledgements

We thank the *Dutch Ministry of Infrastructure and Water Management, Rijkswaterstaat* for providing insight into the cost structure of motorways, and the *Bavarian State Ministry for Housing, Construction and Transport* for providing the data on flood damage in Deggendorf. Deltares colleagues Thomas Bles, Ana Laura Costa and Dennis Wagenaar contributed to shaping the new damage curves. Aoife O'Connor assisted in collecting data on road construction costs.

References

Albano, R., Mancusi, L., Sole, A. and Adamowski, J.: FloodRisk: a collaborative, free and open-source software for flood risk analysis, Geomatics, Nat. Hazards Risk, 8(2), 1812–1832, doi:10.1080/19475705.2017.1388854, 2017.

Alfieri, L., Salamon, P., Bianchi, A., Neal, J., Bates, P. and Feyen, L.: Advances in pan-European flood hazard mapping, Hydrol. Process., 28(13), 4067–4077, doi:10.1002/hyp.9947, 2014.

Alfieri, L., Feyen, L., Dottori, F. and Bianchi, A.: Ensemble flood risk assessment in Europe under high end climate scenarios, Glob. Environ. Chang., 35, 199–212, doi:10.1016/j.gloenvcha.2015.09.004, 2015.

Alfieri, L., Feyen, L. and Di Baldassarre, G.: Increasing flood risk under climate change: a pan-European assessment of the benefits of four adaptation strategies, Clim. Change, 136(3–4), 507–521, doi:10.1007/s10584-016-1641-1, 2016a.

Alfieri, L., Feyen, L., Salamon, P., Thielen, J., Bianchi, A., Dottori, F. and Burek, P.: Modelling the socio-economic impact of river floods in Europe, Nat. Hazards Earth Syst. Sci., 16(6), 1401–1411, doi:10.5194/nhess-16-1401-2016, 2016b.

Alfieri, L., Dottori, F., Betts, R., Salamon, P. and Feyen, L.: Multi-Model Projections of River Flood Risk in Europe under Global Warming, Climate, 6(1), 6, doi:10.3390/cli6010006, 2018.

Amadio, M., Mysiak, J., Carrera, L. and Koks, E.: Improving flood damage assessment models in Italy,

Nat. Hazards, 82(3), 2075–2088, doi:10.1007/s11069-016-2286-0, 2016.

Amadio, M., Rita Scorzini, A., Carisi, F., Essenfelder, H. A., Domeneghetti, A., Mysiak, J. and Castellarin, A.: Testing empirical and synthetic flood damage models: The case of Italy, Nat. Hazards Earth Syst. Sci., 19(3), 661–678, doi:10.5194/nhess-19-661-2019, 2019.

615 Archondo-Callao, R., Roads works costs per km from World Bank Reports (presentation). April, 2000.

Arnell, N. W. and Gosling, S. N.: The impacts of climate change on river flood risk at the global scale, Clim. Change, 134(3), 387–401, doi:10.1007/s10584-014-1084-5, 2016.

Barrington-Leigh, C. and Millard-Ball, A.: The world's user-generated road map is more than 80% complete, PLoS One, 12(8), 1–20, doi:10.1371/journal.pone.0180698, 2017.

620 Bates, P. D., Horritt, M. S., & Fewtrell, T. J.: A simple inertial formulation of the shallow water equations for efficient two-dimensional flood inundation modelling. J. Hydrol. 387(1-2), 33-45, doi: 10.1016/j.jhydrol.2010.03.027

Blanc-Brude, F., Goldsmith, H. and Välilä, T.: Ex Ante Construction Costs in the European Road Sector: A Comparison of Public-Private Partnerships and Traditional Public Procurement (Economic and
625 Financial Report 2006/01), Europ. Invest. Bank, Kirchberg., 2006.

Bles, T., Bessembinder, J., Chevreuil, M., Danielsson, P., Falemo, S., Venmans, A., Ennesser, Y., Löfroth, H.: Climate change risk assessment and adaptation for roads – results of the ROADAPT project, in: Transportation Research Procedia 14, doi:10.1016/j.trpro.2016.05.041, 6th Transport Research Arena, Warsaw, Poland, 18-21 April 2016, 58-67, 2016.

630 Bouwer, L., Capriolo, A., Chiabai,. A., Foudi, S., Garrote, L., Harmackova, Z.V., Iglesias, A., Jeuken, A., Olazabal, M., Spadaro, J., Taylor, T., Zandersen, M.: Upscaling the impacts of climate change in different sectors and adaptation strategies, in: Adapting to climate change in Europe, edited by: Sanderson, H., Hilden, M., Russel, D., Penha-Lopes, G., Capriolo, A., Elsevier, Amsterdam, The Netherlands, 173-243, doi: 10.1016/B978-0-12-849887-3.00001-0, 2018.

635 Bubeck, P., Dillenardt, L., Alfieri, L., Feyen, L., Thieken, A. H. and Kellermann, P.: Global warming to increase flood risk on European railways, Clim. Change, 155(1), 19–36, doi:10.1007/s10584-019-02434-5, 2019.

Büttner, G., Soukup, T. and Kosztra, B.: CLC2012. Addendum to CLC2006 Technical Guidelines, European Environment Agency, Copenhagen, Denmark, 35 pp., 2014.

640 Carisi, F., Schröter, K., Domeneghetti, A., Kreibich, H. and Castellarin, A.: Development and assessment of uni- and multivariable flood loss models for Emilia-Romagna (Italy), Nat. Hazards Earth Syst. Sci., 18(7), 2057–2079, doi:10.5194/nhess-18-2057-2018, 2018.

Carruthers, R.: What prospects for transport infrastructure and impacts on growth in southern and eastern Mediterranean countries?, MEDPRO report No. 3, 2013.

645 Dankers, R. and Feyen, L.: Climate change impact on flood hazard in Europe: An assessment based on high-resolution climate simulations, J. Geophys. Res. Atmos., 113(19), 1–17, doi:10.1029/2007JD009719, 2008.

Doll, C., Klug, S. and Enei, R.: Large and small numbers: options for quantifying the costs of extremes on transport now and in 40 years, Nat. Hazards, 72(1), 211–239, doi:10.1007/s11069-013-0821-9,
650 2014.

Dottori, F., Martina, M. L. V. and Figueiredo, R.: A methodology for flood susceptibility and vulnerability analysis in complex flood scenarios, J. Flood Risk Manag., 11, S632–S645, doi:10.1111/jfr3.12234, 2018a.

Dottori, F., Szewczyk, W., Ciscar, J. C., Zhao, F., Alfieri, L., Hirabayashi, Y., Bianchi, A., Mongelli, I., Frieler, K., Betts, R. A. and Feyen, L.: Increased human and economic losses from river flooding with anthropogenic warming, Nat. Clim. Chang., 8(9), 781–786, doi:10.1038/s41558-018-0257-z, 2018b.

Dottori, F., Mentaschi, L., Bianchi, A., Alfieri, L., and Feyen L.: Adapting to rising river flood risk in the EU under climate change, Publications Office of the European Union, Luxembourg, doi: 10.2760/14505, 2020.

Enei, R., Doll, C., Klug, S., Partzsch, I., Sedlacek, N., Kiel, J., Nesterova, N., Rudzikaite, L., Papanikolaou, A. and Mitsakis, V.: Weather Extremes: Assessment of Impacts on Transport Systems and Hazards for European Regions. Deliverable 2: Vulnerability of Transport systems., Karlsruhe, Germany, 2011.

ECA: Are EU Cohesion Policy funds well spent on roads? Special Report No 5/2013, European Court of Auditors, Luxembourg, Luxembourg, https://doi.org/10.2865/71435, 2013.

EEA: The thematic accuracy of Corine land cover 2000 – assessment using LUCAS, Technical report No 7/2006, European Environment Agency, Copenhagen, Denmark, 2006.

Eurostat: Real GDP per capita, Statistical Office of the European Union, sdg_08_10, 2019.

Federal Ministry of Transport and Digital Infrastructure: Verkehrsinvestitionsbericht für das berichtsjahr 2016, Berlin, Germany, 2016.

Gil, J. and Steinbach, P.: From flood risk to indirect flood impact: Evaluation of street network performance for effective management, response and repair, WIT Trans. Ecol. Environ., 118, 335–344, doi:10.2495/FRIAR080321, 2008.

Hackl, J., Heitzler, M., Lam, J. C., Adey, B. and Hurni, L.: Deliverable 4.2 of the INFRARISK project (Novel indicators for identifying critical infrastructure at risk from natural hazards), Zürich, Switzerland, 2016.

Hackl, J., Lam, J. C., Heitzler, M., Adey, B. T., & Hurni, L.: Estimating network related risks: A methodology and an application in the transport sector, Nat. Hazards Earth Syst. Sci., 18(8), 2273–2293, doi: 10.5194/nhess-18-2273-2018, 2018.

Heralova, R. S., Hromada, E. and Johnston, H.: Cost structure of the highway projects in the Czech Republic, Procedia Eng., 85, 222–230, doi:10.1016/j.proeng.2014.10.547, 2014.

Heralova, R. S., Hromada, E. and Johnston, H.: Cost structure of the highway projects in the Czech Republic, Procedia Eng., 85, 222–230, doi:10.1016/j.proeng.2014.10.547, 2014.

Hirabayashi, Y., Mahendran, R., Koirala, S., Konoshima, L., Yamazaki, D., Watanabe, S., Kim, H. and Kanae, S.: Global flood risk under climate change, Nat. Clim. Chang., 3(9), 816–821, doi:10.1038/nclimate1911, 2013.

Huizinga, H. J.: Flood damage functions for EU member states, HKV Consultants, Lelystad, The Netherlands, 2007.

Huizinga, J., de Moel, H. and Szewczyk, W.: Global flood depth-damage functions. Methodology and database with guidelines, Publications Office of the European Union, Luxembourg, doi: 10.2760/16510, 2017.

International Sava River Basin Commission: Preliminary Flood Risk Assessment in the Sava River Basin, Zagreb, Croatia, 2014.

Jongman, B., Kreibich, H., Apel, H., Barredo, J. I., Bates, P. D., Feyen, L., Gericke, A., Neal, J., Aerts, J. C. J. H. and Ward, P. J.: Comparative flood damage model assessment: Towards a European approach, Nat. Hazards Earth Syst. Sci., 12(12), 3733–3752, doi:10.5194/nhess-12-3733-2012, 2012.

Jongman, B., Hochrainer-Stigler, S., Feyen, L., Aerts, J. C. J. H., Mechler, R., Botzen, W. J. W., Bouwer, L. M., Pflug, G., Rojas, R. and Ward, P. J.: Increasing stress on disaster-risk finance due to large floods, Nat. Clim. Chang., 4(4), 264–268, doi:10.1038/nclimate2124, 2014.

Jonkman, S. N., and Kelman, I.: An Analysis of the Causes and Circumstances of Flood Disaster Deaths. Disasters 29(1), 75-79, doi: 10.1111/j.0361-3666.2005.00275.x, 2005

van der Knijff, J. M., Younis, J. and De Roo, A. P. J.: LISFLOOD: a GIS-based distributed model for river basin scale water balance and flood simulation, Int. J. Geogr. Inf. Sci., 24(2), 189–212, doi:10.1080/13658810802549154, 2010.

Koks, E. E., Rozenberg, J., Zorn, C., Tariverdi, M., Vousdoukas, M., Fraser, S. A., Hall, J. W. and Hallegatte, S.: A global multi-hazard risk analysis of road and railway infrastructure assets, Nat. Commun., 10(1), 1–11, doi:10.1038/s41467-019-10442-3, 2019.

Kreibich, H., Piroth, K., Seifert, I., Maiwald, H., Kunert, U., Schwarz, J., Merz, B. and Thieken, A. H.: Is flow velocity a significant parameter in flood damage modelling?, Nat. Hazards Earth Syst. Sci., 9(5), 1679–1692, doi:10.5194/nhess-9-1679-2009, 2009.

Kron, W.: Flood Risk = Hazard x Values x Vulnerability, Water Int., 30(1), 58–68, doi:10.1080/02508060508691837, 2005.

Kundzewicz, Z. W., Krysanova, V., Dankers, R., Hirabayashi, Y., Kanae, S., Hattermann, F. F., Huang, S., Milly, P. C. D., Stoffel, M., Driessen, P. P. J., Matczak, P., Quevauviller, P. and Schellnhuber, H. J.: Differences in flood hazard projections in Europe–their causes and consequences for decision making, Hydrol. Sci. J., 62(1), 1–14, doi:10.1080/02626667.2016.1241398, 2017.

Lamb, R., Garside, P., Pant, R. and Hall, J. W.: A Probabilistic Model of the Economic Risk to Britain's Railway Network from Bridge Scour During Floods, Risk Anal., 39(11), doi:10.1111/risa.13370, 2019.

Lincke, D., Hinkel, H., van Ginkel, K., Jeuken, A., Botzen, W., Tesselaar, M., Scoccimarro, E., Ignjacevic, P.: Impacts on infrastructure, built environment and transport, Deliverable 2.3 of the COACCH project, 78 pp., 2019.

Lugeri, N., Kundzewicz, Z. W., Genovese, E., Hochrainer, S. and Radziejewski, M.: River flood risk and adaptation in Europe-assessment of the present status, Mitig. Adapt. Strateg. Glob. Chang., 15(7), 621–639, doi:10.1007/s11027-009-9211-8, 2010.

Meneses, B. M., Pereira, S. and Reis, E.: Effects of different land use and land cover data on the landslide susceptibility zonation of road networks, Nat. Hazards Earth Syst. Sci., 19(3), 471–487, doi:10.5194/nhess-19-471-2019, 2019.

Merz, B., Kreibich, H., Schwarze, R. and Thieken, A.: Assessment of economic flood damage, Nat. Hazards Earth Syst. Sci., 10(8), 1697–1724, doi:10.5194/nhess-10-1697-2010, 2010.

de Moel, H., van Alphen, J., & Aerts, J. C. J. H.: Flood maps in Europe - methods, availability and use, Nat. Hazards Earth Syst. Sci., 9(2), 289–301, doi:10.5194/nhess-9-289-2009, 2009.

de Moel, H. and Aerts, J. C. J. H.: Effect of uncertainty in land use, damage models and inundation depth on flood damage estimates, Nat. Hazards, 58(1), 407–425, doi:10.1007/s11069-010-9675-6, 2011.

de Moel, H., Jongman, B., Kreibich, H., Merz, B., Penning-Rowsell, E. and Ward, P. J.: Flood risk
735 assessments at different spatial scales, Mitig. Adapt. Strateg. Glob. Chang., 20(6), 865–890, doi:10.1007/s11027-015-9654-z, 2015.

Nijland, H., Wortelboer-van Donselaar, P. M., Korteweg, J. A. C. and Snellen, D.: 'Met de kennis van nu': leren van evalueren Een casestudy: A5 Verlengde Westrandweg, Netherlands Environmental Assessment Agency, The Hague, The Netherlands, 2010.

740 Olsen, A. S., Zhou, Q., Linde, J. J., & Arnbjerg-Nielsen, K.: Comparing methods of calculating expected annual damage in urban pluvial flood risk assessments, Water, 7(1), 255–270, doi.org/10.3390/w7010255, 2015.

OpenStreetMap contributors: http://openstreetmap.org, Europe dump of 7 januari 2019.

Paprotny, D., Sebastian, A., Morales-Nápoles, O. and Jonkman, S. N.: Trends in flood losses in Europe
745 over the past 150 years, Nat. Commun., 9(1), doi:10.1038/s41467-018-04253-1, 2018.

Peduzzi, P., Dao, H., Herold, C. and Mouton, F.: Assessing global exposure and vulnerability towards natural hazards: the Disaster Risk Index, Nat. Hazards Earth Syst. Sci., 9(4), 1149–1159, doi:10.5194/nhess-9-1149-2009, 2009.

Prahl, B. F., Boettle, M., Costa, L., Kropp, J. P. and Rybski, D.: Damage and protection cost curves for
750 coastal floods within the 600 largest European cities, Sci. Data, 5(1), 180034, doi:10.1038/sdata.2018.34, 2018.

Pregnolato, M.: Bridge safety is not for granted – A novel approach to bridge management, Eng. Struct., 196, 109193, doi:10.1016/j.engstruct.2019.05.035, 2019.

Pryzluski, V., Hallegatte, S., Tomozeiu, R., Cacciamani, C., Pavan, V. and Doll, C.: Weather Trends and
755 Economy-Wide Impacts (Deliverable 1 within the research project WEATHER (Weather Extremes: Impacts on Transport Systems and Hazards for European Regions), Karlsruhe, Germany, 2012.

Reese, S., Markau, H., Sterr, H.: Mikroskalige Evaluation der Risiken in überflutungsgefährdeten Küstenniederungen, Forschungs- und Technologiezentrum Westküste, E34893, Kiel, Germany, 2003.

Rogowsky, W.: Erfahrungsbericht vor Ort beim Hochwasser 2013 in Bayern, Internationales
760 Wasserbau-Symposium Aachen (IWASA), pp. 1–10, Aachen, Germany, 2016.

Rosina, K., Batista e Silva, F., Vizcaino, P., Marín Herrera, M., Freire, S. and Schiavina, M.: Increasing the detail of European land use/cover data by combining heterogeneous data sets, Int. J. Digit. Earth, 8947, doi:10.1080/17538947.2018.1550119, 2018.

Scussolini, P., Aerts, J. C. J. H., Jongman, B., Bouwer, L. M., Winsemius, H. C., De Moel, H., and Ward,
765 P. J.: FLOPROS: an evolving global database of flood protection standards, Nat. Hazards Earth Syst. Sci., 16(5), 1049–1061. doi:10.5194/nhess-16-1049-2016, 2016.

Serinaldi, F. and Kilsby, C. G.: A Blueprint for Full Collective Flood Risk Estimation: Demonstration for European River Flooding, Risk Anal., 37(10), 1958–1976, doi:10.1111/risa.12747, 2017.

Sohn, J.: Evaluating the significance of highway network links under the flood damage: An
770 accessibility approach, Transport Res A-Pol, 40(6), 491-506, doi: 10.1016/j.tra.2005.08.006, 2006.

Strappazzon, Q. and Pierlot, D.: Stratégie locale de Gestion du Risque Inondation: Grenoble – Voiron., Grenoble, France, 2017.

Thieken, a. H., Ackermann, V., Elmer, F., Kreibich, H., Kuhlmann, B., Kunert, U., Maiwald, H., Merz, B., Müller, M., Piroth, K., Schwarz, J., Schwarze, R., Seifert, I. and Seifert, J.: Methods for the evaluation of direct and indirect flood losses, in RIMAX Contributions at the 4th International Symposium on Flood Defence (ISFD4), pp. 1–10, 2009.

Thielen, J., Bartholmes, J., Ramos, M.-H. and de Roo, A.: The European Flood Alert System – Part 1: Concept and development, Hydrol. Earth Syst. Sci., 13(2), 125–140, doi:10.5194/hess-13-125-2009, 2009.

Vennapusa, P. K. R., White, D. J. and Miller, D. K.: Western Iowa Missouri River Flooding — Geo-Infrastructure Damage Assessment, Repair and Mitigation Strategies, Iowa State Univ., InTrans Project Reports 97, 2013.

Ward, P. J., Jongman, B., Weiland, F. S., Bouwman, A., van Beek, R., Bierkens, M. F. P., Ligtvoet, W. and Winsemius, H. C.: Assessing flood risk at the global scale: Model setup, results, and sensitivity, Environ. Res. Lett., 8(4), 44019, doi:10.1088/1748-9326/8/4/044019, 2013.

Winsemius, H. C., Van Beek, L. P. H., Jongman, B., Ward, P. J. and Bouwman, A.: A framework for global river flood risk assessments, Hydrol. Earth Syst. Sci., 17(5), 1871–1892, doi:10.5194/hess-17-1871-2013, 2013.